DNA Mesophases Induced by Spermidine: Structural Properties and Biological Implications

Juan Pelta,* Dominique Durand,# Jean Doucet,# and Françoise Livolant*
*Laboratoire de Physique des Solides, and Laboratoire pour l'Utilisation du Rayonnement Electromagnétique, Université Paris Sud, 91405 Orsay Cedex, France

ABSTRACT Conditions of formation of DNA aggregates by the addition of spermidine were determined with 146 base pair DNA fragments as a function of spermidine and NaCl concentration. Two different phases of spermidine-DNA complexes are obtained: a cholesteric liquid crystalline phase with a large helical pitch, with interhelix distances ranging from 31.6 to 32.6 Å, and a columnar hexagonal phase with a restricted fluidity in which DNA molecules are more closely packed (29.85 ± 0.05 Å). In both phases, the DNA molecule retains its B form. These phases are always observed in equilibrium with the dilute isotropic solution, and their phase diagram is defined for a DNA concentration of 1 mg/ml. DNA liquid crystalline phases induced by spermidine are compared with the DNA mesophases already described in concentrated solutions in the absence of spermidine. We propose that the liquid crystalline character of the spermidine DNA complexes is involved in the stimulation of the functional properties of the DNA reported in numerous experimental articles, and we discuss how the nature of the phase could regulate the degree of activity of the molecule.

INTRODUCTION

In a cell nucleus, all of the macromolecular species taken together occupy a substantial fraction of the fluid volume, and the cell nucleus must be considered as a macromolecular crowded medium (Minton, 1981). One may roughly estimate that the local DNA concentration is never lower than 50 mg/ml and can reach concentrations up to about 400 mg/ml. These crowded conditions cannot be neglected in the understanding of the functional properties of DNA molecules. Nevertheless, up to now, the organization of DNA in these condensed and complex structures remains largely unknown.

In vitro, different methods can be used to create model systems to study the ordering of DNA molecules in this range of concentration. Among them, two approaches may be considered as being closely related to the mechanisms involved in vivo.

Confinement of DNA to a very small volume

The increase in DNA concentration can be achieved by a progressive dehydration of the solution as first shown by Robinson (1961). Under such conditions, DNA forms multiple liquid crystalline phases, depending on the polymer concentration. These states are now quite well understood. The dilute DNA solution is isotropic below a concentration that depends on the length of the DNA fragments. Then the solution orders into a cholesteric liquid crystalline phase (Livolant, 1986; Strzelecka et al., 1987; Rill et al., 1991; Leforestier and Livolant, 1993) through the formation of double twist configurations (either precholesteric states (Livolant, 1987) or blue phases (Leforestier and Livolant, 1994)). When the concentration increases, the cholesteric phase transforms into a columnar hexagonal phase with a two-dimensional order (Luzzati and Nicolaieff, 1959, 1963; Livolant and Bouligand, 1986; Livolant et al., 1989; Livolant, 1991), which turns itself into a true three-dimensional crystal, first hexagonal and then orthorhombic. This evolution can be monitored by x-ray diffraction with 50-nm DNA fragments, allowing the authors to measure the interhelix distances and to calculate the DNA concentrations at which the phase transitions occur (Durand et al., 1992).

Condensation of DNA can also be obtained by the addition of a neutral polymer such as polyethylene glycol in the presence of monovalent salts. The two polymers are incompatible, and they segregate into different phases. The polymer and salt-induced DNA, usually characterized by circular dichroism properties (PSI-type CD spectra) (Lerman, 1974; Maniatis et al., 1974), corresponds to liquid crystalline phases of DNA (Livolant, 1986; Livolant and Bouligand, 1986; Evdokimov et al., 1988). The osmotic pressure exerted on the DNA sample can be modulated by varying the neutral polymer concentration, leading to a progressive decrease in the interhelix spacing (Rau et al., 1984: Podgornik et al., 1996) and therefore to different liquid crystalline phases similar to those described with the other method.

Neutralization of the DNA molecule by polycations or basic proteins

DNA condensation can also be achieved by neutralization of the charges along the DNA molecule as theoretically postulated by Manning (1978) (Bloomfield et al., 1994). Collapse or aggregation of DNA is obtained with polycationic molecules: ions (polyamines, cobalt hexamine), polypeptides (polylysine, polyhistidine), or proteins (his-

Received for publication 12 September 1995 and in final form 8 April 1996.
Address reprint requests to Dr. Françoise Livolant, Laboratoire de Physique des Solides, Bât. 510, Université Paris Sud, 91405 Orsay Cedex, France. Tel.: 69-41-53-92; Fax: 69-41-60-87; E-mail: livolant@lps.u-psud.fr.

0006-3495/96/07/48/16 $2.00

tones H1). These agents, which interact directly with the DNA molecules (in contrast with neutral polymers which are excluded from the DNA phase), induce the formation of DNA aggregates that can be sedimented by centrifugation.

Among these different agents, we were mainly interested in polyamines, which are organic polycations encountered in millimolar concentrations in all cell types as well in prokaryotes and eukaryotes. They are involved in numerous cellular processes, including replication and protein synthesis, and in the activity of numerous enzymatic systems (Tabor and Tabor, 1984). Moreover, they are also frequently used in vitro to stimulate a number of enzymatic activities involving the DNA molecule. Condensation of DNA by polyamines has been extensively investigated (for a review, see Bloomfield, 1991). In extremely dilute solution (less than 1 to about 10 μg/ml), a monomolecular collapse (when only one molecule is involved) or the formation of microaggregates can occur, and polyamine-DNA complexes form either tores (Gosule and Schellman, 1976; Chattoraj et al., 1978; Baeza et al., 1987) or spheres (Chattoraj et al., 1978). In dilute solutions (about 1 mg/ml), the aggregates are large enough to sediment in a pellet (Damaschun et al., 1978).

We reported recently that a liquid crystalline ordering of DNA can be induced by spermidine (Sikorav et al., 1994). Two phases were obtained in equilibrium. The aim of the present work is to investigate the precise nature of these two phases, to determine the range of conditions under which they are formed, and to compare these data with the classical liquid crystalline DNA phases. Finally, we will discuss from a biological point of view the potential interest of these DNA mesophases induced by spermidine.

MATERIALS AND METHODS

Materials

DNA fragments (500 Å) were prepared as described by Sikorav et al. (1994) by selective digestion of calf thymus chromatin with micrococcal nuclease (Strzelecka and Rill, 1987). The ratio OD_{260}/OD_{280} was 1.85, indicating a protein-free preparation. To assess the polydispersity of the fragments, a sample was 5'-end-labeled with T4 DNA kinase using γ^{32}P-ATP. The length of the fragments was determined by electrophoresis on polyacrylamide gels. Quantification of the radioactive bands was carried out on a PhosphoreImager (Molecular Dynamics). The sample contains 50% of 146 ($\pm$7) base pair fragments. In view of the polydispersity of the sample, part of the DNA was further fractionated according to the method described by Lerman et al. (1976): successive aliquots of absolute ethanol were added to the TE solution (10 mM Tris, 1 mM EDTA, pH 7.6) containing 5 mg/ml DNA and 0.3 M ammonium acetate. DNA molecules were sequentially precipitated according to their length, from longer to shorter fragments. We did not notice any differences in the results between the two samples, except small variations of the amount of DNA precipitated in the pellet.

Spermidine (3 HCl; Fluka) was prepared as a stock solution at a concentration of 100 mg/ml (392 mM) in 10 mM TE buffer (pH 7.6).

Aggregation of DNA

Stock DNA solutions (25 mg/ml or more) were prepared in TE buffer (10 mM Tris, 1 mM EDTA, pH 7.6) containing NaCl (40 mM or 250 mM) and extensively dialyzed at 4°C against the same solution. An aliquot of the DNA solution was diluted with the same buffer, and spermidine was added to reach the final concentrations of 1 mg/ml DNA and 1 to 180 mM spermidine. The NaCl concentration was adjusted to values ranging from 4 to 200 mM. A second set of experiments was performed under the same conditions plus 10 mM $MgCl_2$. After vortexing, the samples were left at room temperature for 15 min and centrifuged for 7 min at 11,300 $\times$ g. The amount of DNA remaining in the supernatant (soluble fraction) was determined by measuring the absorbance at 260 nm, after dilution in TE added with NaCl to keep the concentration of monovalent cations constant. The errors in the measurements were estimated to be less than 5%, except for a few experimental points corresponding to high spermidine concentrations, for which a larger dispersion of the measurements was observed. All experiments were performed at room temperature.

Polarizing microscopy

The DNA pellet was recovered and deposited between slide and coverslip (previously cleaned with ethanol and rinsed in distilled water). The coverslip was sealed with DPX, a neutral solution of polystyrene and plasticizers in xylene (Fluka) to prevent dehydration of the preparation. Textures were allowed to stabilize for a few minutes to a few hours. Observations were made in a polarizing Optiphot Nikon microscope. In some cases, a λ plate was inserted between crossed polars to analyze the orientations of the DNA molecule in particular domains.

X-ray diffraction experiments

The pellets were introduced into quartz capillaries 1 mm in diameter previously filled with the supernatant. In some cases, a slight orientation of DNA fragments parallel to the axis of the capillary was obtained during the introduction of the specimen. A few samples were centrifuged (400 to 900 $\times$ g for 3 to 30 min) to obtain a better orientation of DNA helices.

The x-ray scattering experiments were carried out using the synchrotron radiation source DCI of LURE (Orsay, France) on station D43. A single bent Si monochromator (111 reflection) was used to select the wavelength 1.27 Å and to focus the beam. The size of the beam was limited by a collimator with a circular aperture 0.5 mm in diameter. The detection system consists of phosphor image plates, which are scanned in two dimensions on the Molecular Dynamics PhosphorImager 400E with a pixel size of (0.172 $\times$ 0.172) μm^2. The parasitic scattering arising from the capillary and the air is separately measured and then subtracted from the patterns. In the case of isotropic diagrams, the scattering intensity was integrated along circles and reported as a function of the magnitude of the scattering vector $s = 2 \sin \theta/\lambda$.

Temperature experiments

The effects of temperature on the supramolecular organization of the condensed aggregates was investigated on a biphasic sample (DNA 1 mg/ml, spermidine 30 mM, NaCl 25 mM). For polarizing microscopy, preparations were sealed carefully with DPX and settled in a Mettler stage. The temperature was varied at a rate of 1 or 2°C/min from 20 to 65°C for a few cycles, and the experiment was repeated with different samples. Cycles of temperature were also performed in sealed Eppendorf tubes as detailed in the Results.

Dilution experiments

For dilution experiments, DNA was dissolved in TE buffer at a concentration of 5 or 27 mg/ml and dialyzed extensively against NaCl 250 mM, NaCl 250 mM + $MgCl_2$ 10 mM, or $MgCl_2$ 125 mM.

Aliquots (13 μl) of the DNA solution were mixed with a given volume of the spermidine stock solution to obtain the desired spermidine/DNA ratio (1, 5, or 10) and deposited in a cupel. Precise volumes of distilled water

were then added drop by drop under the microscope. To prevent dehydration effects at the air interface, the same experiments were also performed between slide and coverslip, with a spacer inserted in between. Distilled water was then added at the edge of the preparation.

Concentration experiments

A drop of the DNA solution with salt and spermidine was allowed to concentrate progressively either in free surface drop or in thin preparation between slide and coverslip. In this case, the coverslip was not sealed and the dehydration was progressive.

In some experiments, after the preparation had reached the desired state of dehydration, a drop of distilled water was added on one edge of the coverslip to produce a gradient of water concentration from one side to the other side of the preparation. These experiments were done under the microscope. After stabilization of the sample, this method allowed us to determine the sequence of the different birefringent phases as a function of the water amount for given DNA/spermidine and DNA/NaCl ratios.

RESULTS

Effects of salts and spermidine on DNA precipitation

In our experiments, the DNA concentration was kept constant at 1 mg/ml. The concentration of the trivalent cation spermidine was varied from 1 mM up to 180 mM under various ionic conditions. The influence of monovalent salts (Na^+) was investigated by varying their concentration from 4 to 200 mM. In addition, the same set of experiments was also performed in the presence of 10 mM divalent cations (Mg^{2+}), which is well known to be present in the cells in millimolar amounts and involved in the cell metabolism. For each experimental point, the amount of DNA sedimented in the pellet was determined. The two sets of data are presented on Figs. 1 and 2.

At moderate salt concentrations (<100 mM NaCl), up to 95% of the DNA is precipitated at low spermidine concentrations (<25 mM spd), in agreement with Osland and Kleppe (1977). Higher spermidine concentrations progressively decrease the amount of DNA precipitated, which was unexpected. The DNA precipitation is nearly suppressed above 70 mM spermidine.

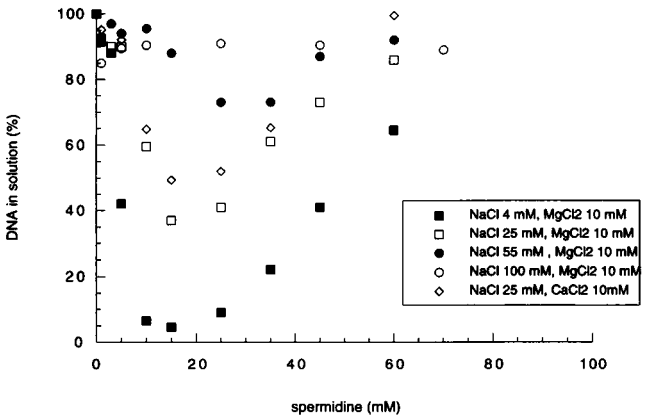

FIGURE 2 Precipitation of DNA as a function of NaCl and spermidine concentrations, in the presence of 10 mM $MgCl_2$ (or 10 mM $CaCl_2$). The overall concentration of DNA was kept constant at 1 mg/ml.

As already observed by Heby and Agrell (1971), precipitation of DNA is completely suppressed in the presence of 100 mM Na^+ (Fig. 1), whatever the concentration of spermidine may be (up to 180 mM). A series of experimental points taken at a fixed concentration of spermidine (25 mM) shows that the suppression of the precipitation occurs progressively when the monovalent salt concentration is increased, leading to a sigmoidal curve (Fig. 3).

The addition of 10 mM Mg^{2+} to the various NaCl concentrations does not modify the overall shape of the curves. It just decreases the amount of precipitated DNA (Fig. 2). This effect is more noticeable when Mg^{2+} is replaced by Ca^{2+} (Fig. 2).

The suppression of precipitation is also observed with 150 mM Mg^{2+} (the threshold concentration may be lower) (not illustrated). These experiments were performed with DNA dialyzed against $MgCl_2$ in TE buffer to get rid of Na^+ ions.

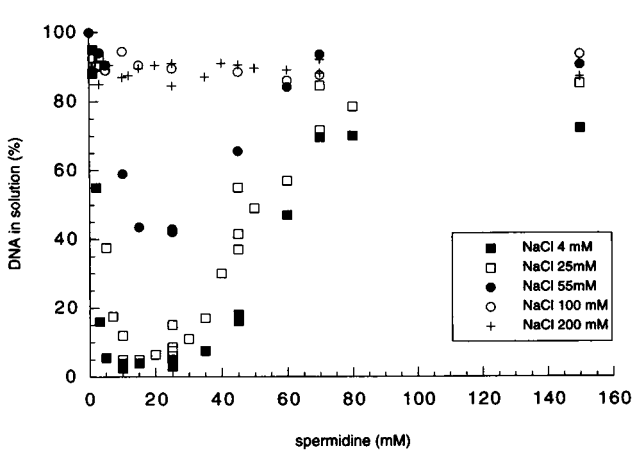

FIGURE 1 Precipitation of DNA as a function of NaCl and spermidine concentrations. The overall concentration of DNA was kept constant at 1 mg/ml.

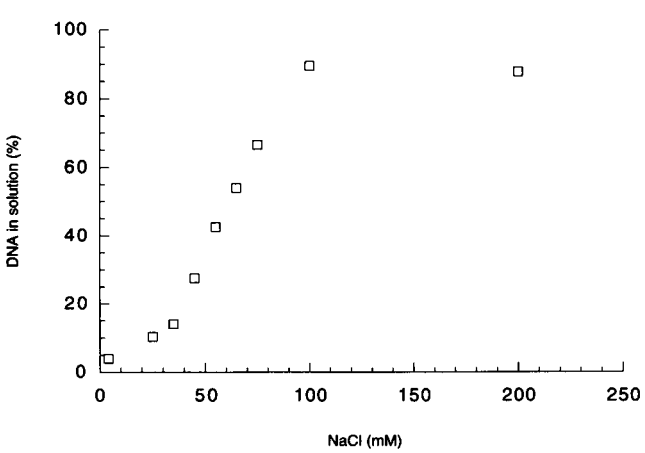

FIGURE 3 Precipitation of DNA as a function of the NaCl concentration for a given spermidine concentration (25 mM). The DNA concentration was equal to 1 mg/ml.

A few experimental points, the characteristics of which are given in Table 1, were chosen to perform structural analyses.

Nature of the DNA precipitates

The DNA pellets show multiple macroscopic aspects, depending on the amounts of spermidine and salts. Their appearance varies from transparent to white opaque. They can be either dense or highly fluid. They are most often extremely sticky, which raises some difficulties in collecting them, either for microscopy or for x-ray diffraction experiments.

Polarizing microscopy

When deposited between slide and coverslip, these aggregates show multiple textures (Figs. 4 and 5), which depend on the nature of the phase but also on the thickness of the preparation. These textures were gathered here in two groups.

Large-pitch cholesteric textures. A cholesteric phase is frequently obtained in the samples, but its characterization is difficult because of the usual absence of classical fingerprint patterns. Instead, birefringent domains are usually observed with a homogeneous illumination (Fig. 4, *a–e*). Nevertheless, the cholesteric nature of this phase is attested by the presence of tear-shaped defects (Fig. 4 *d*), which are characteristic of a cholesteric organization (Bouligand, 1974). Classical fingerprint textures were observed only in thick preparations (0.5 to 1 mm) in rectangle capillary tubes (Vitro Dynamics) (not illustrated). The periodicity of the stripes allowed us to measure the helical pitch, which is about 22 μm. This phase is highly fluid and flows spontaneously under the microscope.

Droplets of this cholesteric phase are sometimes observed to be floating in the dilute isotropic phase (Fig. 4 *a*). The droplets look like slightly twisted nematic spherulites with two singular points corresponding to discontinuities of the molecular orientations at the surface of the sphere. Instead of spheres, the droplets may also be torus-like, with one or a few holes (Fig. 4 *a*).

Sometimes, nematic textures can be seen, as revealed by the presence of two or four branch brush defects (Fig. 4 *b*). These textures, which are quite rare, probably correspond to the previously described cholesteric phase, in which the twist is prevented by anchoring effects on the glass slides.

Numerous isotropic droplets of various sizes may be trapped in this birefringent cholesteric phase (Fig. 4, *a*, *c*, *e*). These droplets usually look spherical when they are isolated (Fig. 4 *c*). They are slightly distorted into "squares" in very thin preparations (Fig. 4 *e*). In particular conditions of preparation of the samples, which will be detailed below, these droplets may be very numerous. Then, they form a three-dimensional network (Fig. 10 *c*).

This large-pitch cholesteric phase is also observed when divalent cations, either Mg^{2+} (Fig. 4 *g*) or Ca^{2+} (not illustrated), are added to the solution. Fingerprint patterns are then usually seen, whatever the thickness of the sample may be (Fig. 4 *g*).

Columnar phase. In most of the pellets, birefringent germs are found flowing with the liquid phase. These germs do not coalesce to form large domains, but remain well individualized, whatever their amount in the sample may be. They are always monocrystalline: DNA molecules present a unidirectional orientation in each of them, as seen by inserting a λ plate between crossed polars, which confers a homogeneous color on each germ (either blue or yellow).

The germs can be dispersed in the cholesteric phase when there are few of them (Fig. 5 *a*). When they are numerous, they stack together into domains showing a more or less uniform orientation of molecules (Fig. 5 *b*). The presence of walls can be seen between such domains. They appear as black lines that follow sinuous paths between the germs. Their presence led us to suspect that a small part of the cholesteric phase may remain between them.

The germs are usually polygonal (Fig. 5, *a* and *b*) and are more or less elongated along one direction. They are 4 to 7 μm wide and up to 20 μm long in most preparations, and the ratio L/l between their length (L) and width (l) varies from about 1.3 to 2.3. Molecules are always normal to the elongation axis of the germ. The germs can be slightly larger if the sample has been heated to 65°C before being stabilized at room temperature.

When the pellet is smeared onto the slide, completely dehydrated and reequilibrated with its supernatant, the germs are still visible but they are then much smaller (2 to 2.5 μm wide) and highly elongated (from 9 to 80 μm long) (with an axial ratio ranging from 5 to 60). These germs are then gathered into elongated domains (Fig. 5 *d*). Molecules remain normal to the elongation axis of the germs (i.e., parallel to the direction of the shear).

In a few cases, textures characteristic of a columnar hexagonal liquid crystal were found (Fig. 5 *c*). The are quite rare; they were observed only for two experimental points,

TABLE 1 Characteristics of the experimental points discussed in the text

Experimental points	NaCl (mM)	$MgCl_2$ (mM)	Spermidine (mM)	Percentage of DNA in the pellet
12	5.7		15.7	97.33
16	5.7	10	15.7	90.6
36	16		43	71.3
102*	4		3	84
106*	4		70	30.5
111	25		25	85
120*	4		15	96
124	25		5	62.5
137*	4		10	97.5
139*	4		45	82
142*	25		25	92.5
143	25		30	89
190*	55		45	34.5
243	4	10	15	95.5

*Samples used for x-ray crystallography.

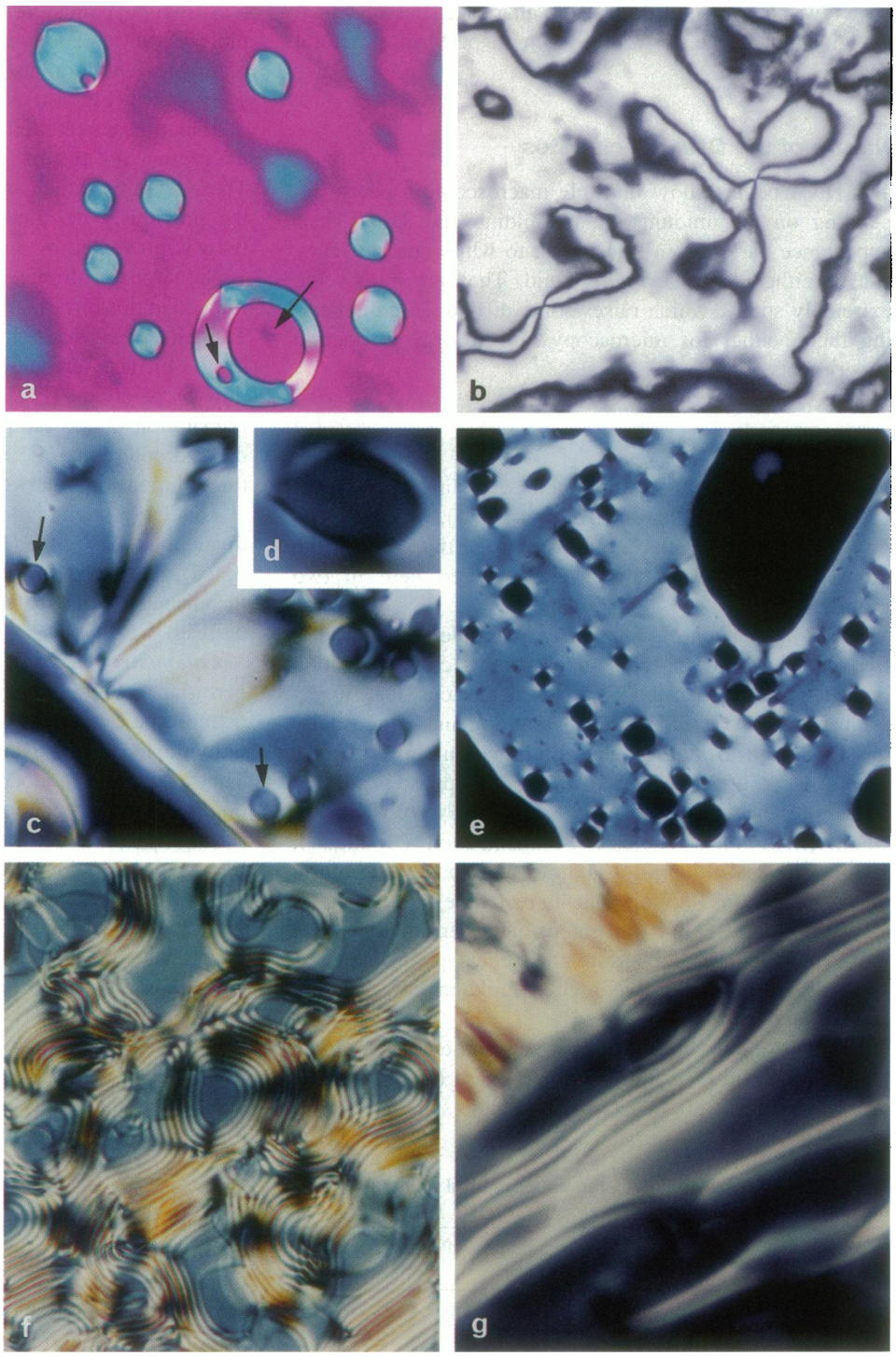

FIGURE 4 Textures of the large-pitch cholesteric phase of spermidine condensed DNA observed in polarizing microscopy. (*a*) Cholesteric droplets in equilibrium with the dilute isotropic phase. The cholesteric droplets may contain bubbles (arrows) (16 mM NaCl, 4 mM spermidine). Crossed polars, λ, ×225. (*b*) Nematic textures in a thin preparation, characterized by black brush defects (10.7 mM NaCl, 7.9 mM spermidine). Crossed polars, ×375. (*c*) Large-pitch cholesteric texture with a few isotropic droplets embedded in the sample (arrows). Crossed polars, ×560. (*d*) Tear-shaped defect line characteristic of a cholesteric structure. Crossed polars, ×760. (*e*) Birefringent texture (probably cholesteric, as in *c* and *d*) containing numerous isotropic bubbles (10.7 mM NaCl, 7.9 mM spermidine). In this case, the preparation is quite thin and the droplets are slightly distorted into rounded squares. Crossed polars, ×150. (*f*) Fingerprint patterns characteristic of the cholesteric phase, obtained by heating the sample (sample 143: 25 mM NaCl, 30 mM spermidine) to a temperature of 30.5°C. Crossed polars, ×225. (*g*) Cholesteric textures with the characteristic fingerprint patterns (5.7 mM NaCl, 10 mM MgCl2, 7.8 mM spermidine). Crossed polars, ×760.

124 and 111, and their presence remains limited to a very small portion of the pellet. These domains present fan-shaped textures with numerous walls of discontinuities radiating around $+\pi$ disclination lines. We checked, by using a quartz first-order retardation plate (λ), that the DNA molecular orientations are curved around these defect lines, which reveals the columnar nature of this phase and rules out the hypothesis of a smectic phase, as demonstrated previously for the concentrated NaDNA samples (Livolant et al., 1989). These domains are much more viscous than the surrounding cholesteric phase. Nevertheless, by squashing them firmly between slide and coverslip, a displacement of the walls (*w*) was obtained, therefore inducing changes in the shape of the overall domains. After being squashed, these domains tend to relax and to recover their original shape.

In one case (point 142) it was possible to squash the isolated germs between slide and coverslip and to transform

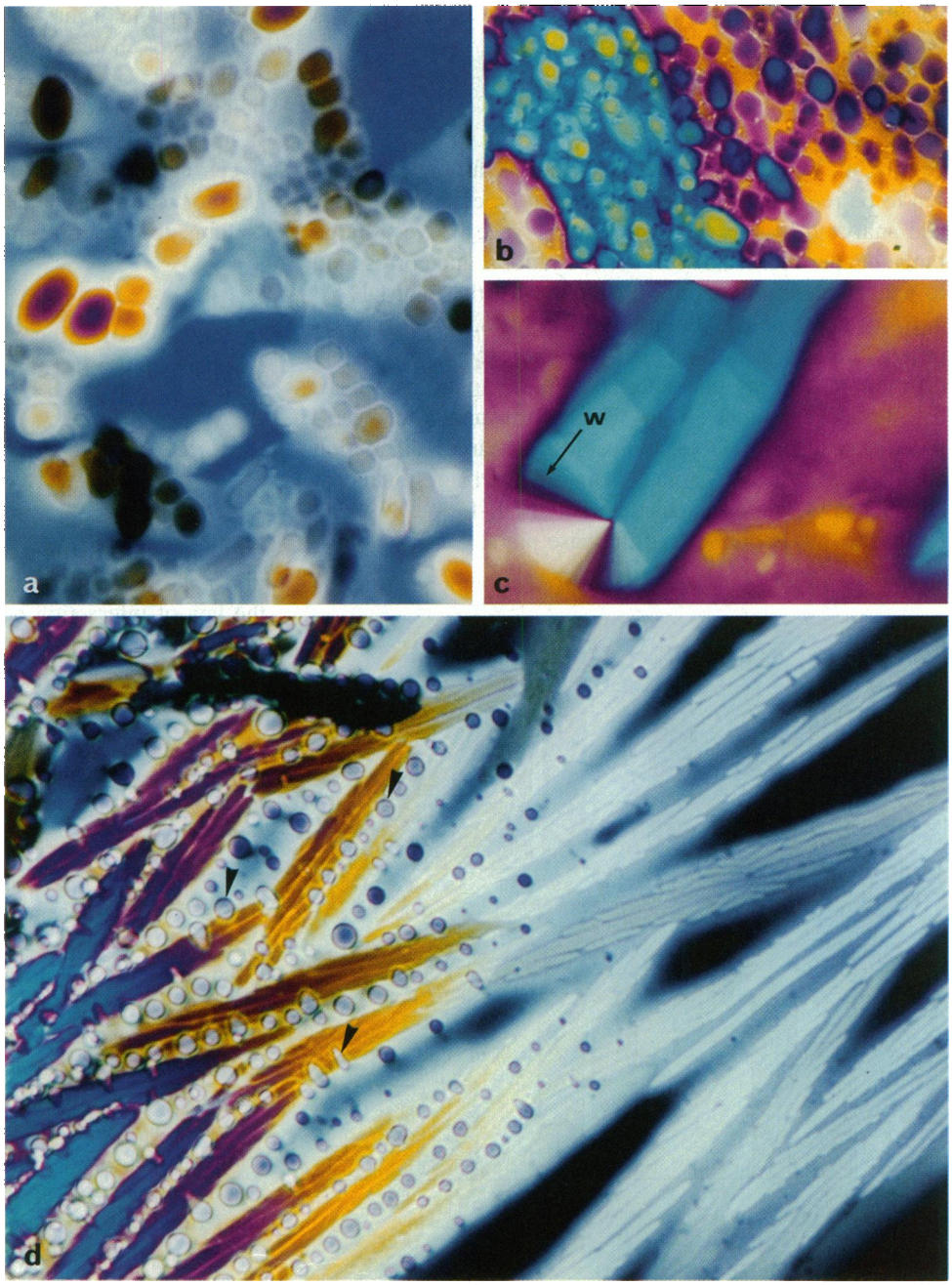

FIGURE 5 Various textures of the columnar phase as seen in polarizing microscopy. (*a*) Birefringent germs in equilibrium with the planar cholesteric phase (16.2 mM NaCl, 43.2 mM spermidine). Crossed polars, ×750. (*b*) Region with numerous columnar germs. The insertion of the λ plate reveals that each germ corresponds to a monodomain. All germs follow the same orientation in a given domain (10.7 mM NaCl, 7.9 mM spermidine). Crossed polars, λ, ×375. (*c*) Columnar hexagonal domain arranged around a $+\pi$ disclination line and showing numerous walls of discontinuities (w) (25 mM NaCl, 5 mM spermidine). Crossed polars, λ, ×690. (*d*) Elongated birefringent domains made of numerous monocrystalline elongated germs in equilibrium with the large-pitch cholesteric phase are obtained by addition of a drop of the mother liquor to a small amount of the aggregate previously smeared and dried. Note the presence of numerous isotropic droplets in equilibrium with the two phases (arrows) (16.2 mM NaCl, 43.2 mM spermidine). Crossed polars, ×1125.

them into these typical columnar textures. This observation strongly supports the hypothesis that germs and columnar textures correspond to a unique columnar phase, with a restricted fluidity limiting strongly the curvature of the columns. Between crossed polars, the illumination of these columnar germs or domains is much higher than the illumination of the cholesteric phase, indicating that the packing of DNA molecules is higher in this phase.

Complex nature of the pellets. The relative amount of the two phases varies with the salt and spermidine concentrations. With the resolution of the polarization microscope, we define three different types of samples:

Pellets purely composed of germs are encountered only for low concentrations of monovalent salts (4 mM Na^+). They usually correspond to a large amount of DNA sedimented in the pellet (more than 85%). As stated previously, we cannot ascertain that they do not contain a very small amount of the cholesteric liquid crystalline phase. Pellets showing only germs were never observed after the addition of Mg^{2+} ions, which increases the ionic strength of the solution.

Purely cholesteric pellets can be found in a large range of NaCl concentrations (4 to 75 mM NaCl), but only for relatively large amounts of spermidine. Furthermore, these pellets contain less than 50% of the total DNA.

Pellets containing both cholesteric liquid crystal and germs correspond to a large range of experimental conditions. The relative amounts of the two phases show strong

variations, which were roughly estimated, as schematized on Fig. 6.

X-ray data

Among the numerous experimental points, a few were chosen to be representative of the different types of aggregates and analyzed by x-ray crystallography. They cover a large range of spermidine and salt concentrations, and correspond to pellets containing from 30% to 96% of the total DNA.

Cholesteric phase. Points 190 and 106, which appear purely cholesteric in the polarizing microscope, give x-ray diffraction patterns characterized in the inner part by a broad and very intense ring, which corresponds to the interaxial spacing of DNA molecules. At larger diffraction angles one observes a much less intense ring situated at about 3.35 Å, which is characteristic of B-form DNA and represents the periodicity of the base pairs.

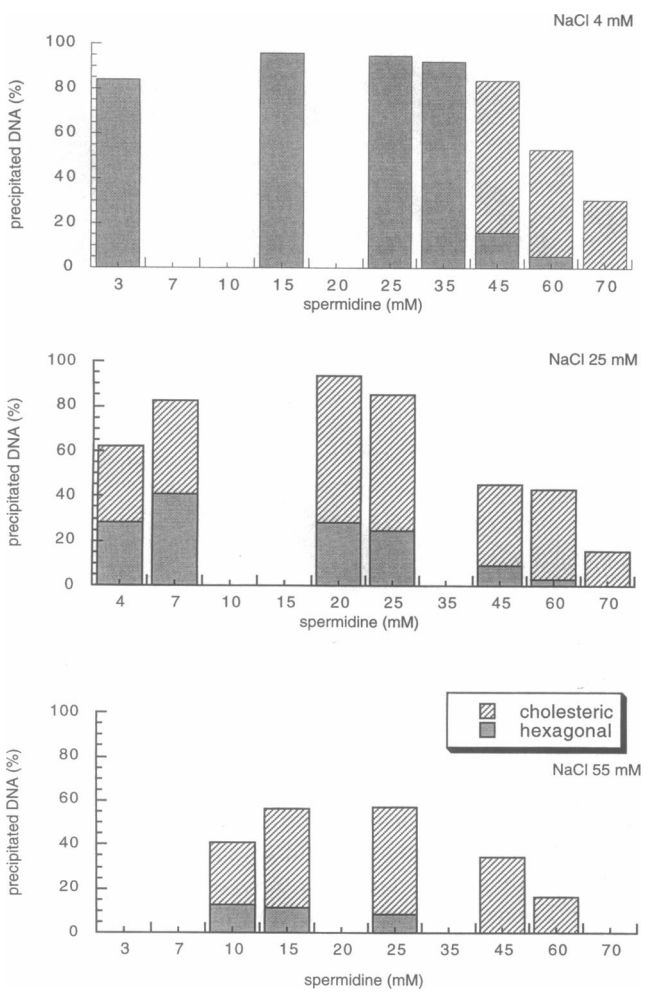

FIGURE 6 The relative amounts of the cholesteric phase (in gray) and of the hexagonal germs (in black) were appreciated qualitatively for numerous experimental points. They are schematically represented here in the form of histograms, the height of which corresponds to the percentage of DNA sedimented in the pellet. Data were collected for three different NaCl concentrations (4, 25, and 55 mM) from top to bottom.

The profile of the scattered intensity $I(s)$ is shown in Fig. 7 for two cholesteric samples, 190 and 106. From the position s_m of the maximum in the scattering curves, s_m being related to the scattering angle θ_m by the relation $s_m = 2 \sin \theta_m/\lambda$, we have deduced an average distance a_m between neighboring DNA helices. The formula that is suitable for isotropic, nematic, or cholesteric phases consisting of long, rodlike molecules is given by

$$2a_m \sin \theta_m = 1.117\lambda.$$

In this way, we find very close values for the intermolecular spacing in samples for points 190 and 106: $a_m = 32.6 \pm 0.2$ Å and 32.2 ± 0.2 Å, respectively. Nevertheless, these values are significantly different; several measurements of the interhelical spacing gave a reproducible difference of about 0.4 Å between the two samples.

Except for the interhelix distance a_m, it is noteworthy that only poor information can be extracted from these diffraction patterns, namely about the structure of the phase and the law of interaction between helices in this phase.

Indeed, the scattered intensity $I(s)$ contains two contributions:

$$I(s) = I_{sup}(s) + I_c(s).$$

The first term is due to the supernatant. The second one is due to the cholesteric phase and can be written as

$$I_c(s) = |F(s)|^2 S_c(s),$$

where $|F(s)|^2$ represents the structure factor of a given DNA helix, and $S_c(s)$ is the structure factor of the assembly of the DNA molecules. Unfortunately, the proportion of supernatant in our specimens is not known. Consequently, we cannot extract from the measured intensity $I(s)$ the part coming from the cholesteric phase and thus obtain the meaningful quantity $S_c(s)$.

Phase with germs. The pellets 102, 120, and 137, purely composed of germs, give identical x-ray patterns. The example shown on Fig. 8 (sample 137 slightly aligned by centrifugation) is typical of DNA molecules oriented parallel to the capillary axis and with a lateral hexagonal arrangement.

In the outer part, a meridian arc located at 3.35 Å is observed. This arc is characteristic of B-DNA helices with base pairs oriented nearly perpendicular to the helix axis and separated by the rise $h = 3.35$ Å.

The inner part of the x-ray patterns mainly displays a sharp arc with a strong equatorial reinforcement. This arc reveals a two-dimensional long-range hexagonal arrangement of the DNA chains in the plane perpendicular to their axes. The parameter a_H of the hexagonal lattice is found to be equal to 29.85 ± 0.05 Å. The other equatorial reflections characteristic of a hexagonal array (spacing ratios with the main reflection in the order $1/\sqrt{3}$, $1/\sqrt{4}$, $1/\sqrt{7}$) are not visible. Their absence is probably due to their very weak structure factor $|F(s)|^2$ when the interhelix distance a_H lies in the range 29.5 Å $\leq a_H \leq 30$ Å.

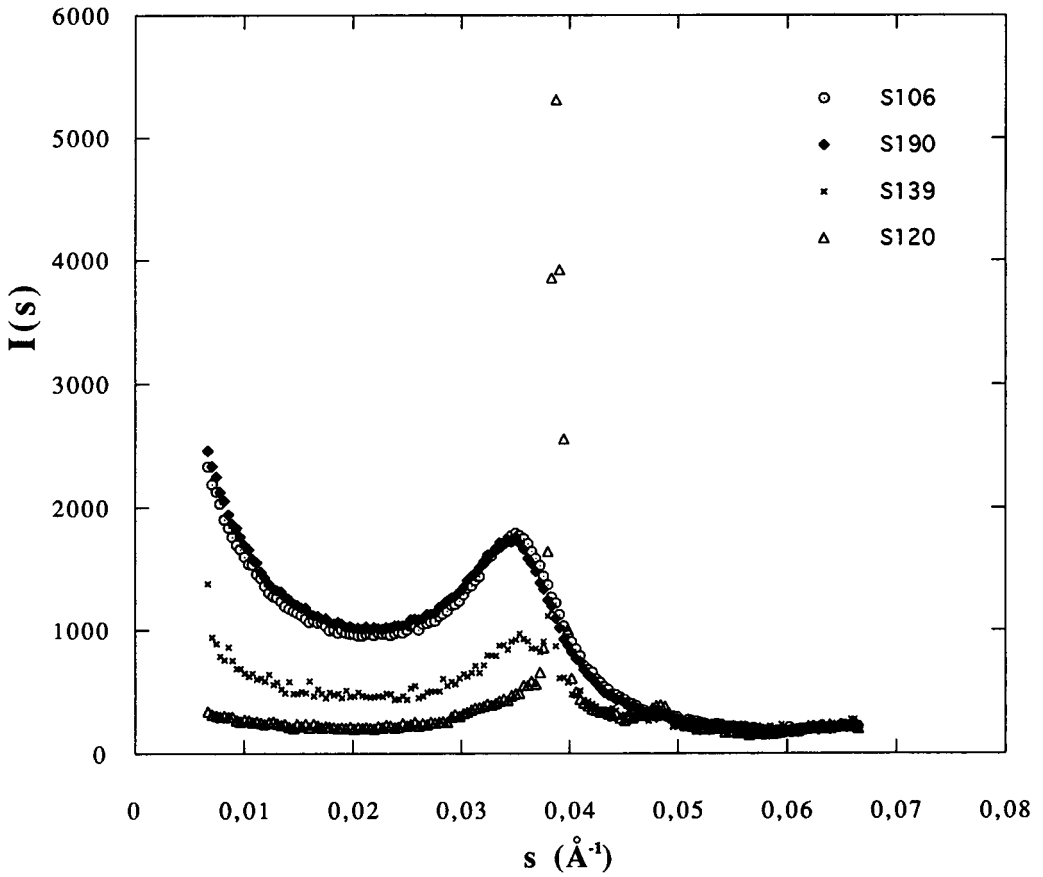

FIGURE 7 Scattered intensity profiles $I(s)$ as a function of $s = 2 \sin \theta/\lambda$ obtained in the cholesteric phase (samples 106 and 190), in the biphasic sample (sample 139), and in the phase with germs (sample 120). The $I(s)$ curve in the phase with germs shows sharp and strong peaks related to the hexagonal arrangement of the DNA chains in the plane perpendicular to their axes. The weak peak located at about $s = 0.047$ Å^{-1} corresponds to the sharp reflections observed along the first layer and associated with the longitudinal order.

One observes also in the inner part of the x-ray patterns four sharp and weak arcs related to the first layer above the equatorial layer. This first layer corresponds to the helix pitch periodicity. Therefore we can deduce the helix pitch P from the position of the weak arcs: $P = 34.7 \pm 0.1$ Å. From the presence of sharp arcs on the first layer, we can conclude that not only a lateral but also a longitudinal order is present between neighboring DNA molecules. Along the second layer (and along the next ones) the intensity is diffuse without sharp arcs, which reveals distortions from the ideal crystalline structure, such that only the short-range longitudinal order is retained. These distortions, also called second kind distortions (Guinier, 1956), are usual in chain molecule assemblies. The obtained diagrams are typical of shift distortions along the axis of the molecules (Vainshtein, 1966, p. 280). As already calculated (Vainshtein, 1966, p. 278), the lth layer line becomes diffuse when $l/P = 0.25/\Delta$, where Δ^2 is the main square fluctuation along the helix axis. In our case, the second layer is diffuse, so $l = 2$ and $\Delta = 4.3$ Å. As a conclusion, our diagrams show a longitudinal order between DNA helices strongly perturbed by displacements of the DNA chains along their axis. The mean square value of these displacements is $\Delta^2 = (4.3 \text{ Å})^2$.

The values of the parameters characteristic of the hexagonal phase, h (the axial translation per residue, commonly called rise), a_H (the interhelix distance), and P (the pitch of the DNA molecule), are the same for the three specimens 102, 120, and 137. From these parameters we can first evaluate the DNA concentration C in the germs defined as the weight of DNA per volume of solution, from the expression

$$C = M_{DNA}/\sigma h,$$

where M_{DNA} is the molecular weight of a base pair and σ is the area of the unit cell in the plane perpendicular to the helix axis, $\sigma = a_H^2\sqrt{3}/2$. It is found that $C \approx 425$ mg/ml. We can also derive the number of nucleotides per helix turn, $n = P/h$, which gives a value $n = 10.35$ very close to the value previously found for condensed DNA phases obtained without spermidine in the same range of DNA concentration (Durand et al., 1992).

Biphasic samples. Points 139 and 142, containing both cholesteric liquid crystal and germs, give x-ray patterns that are identical to the superimposition of the patterns obtained for the phase purely composed of germs and for the pure

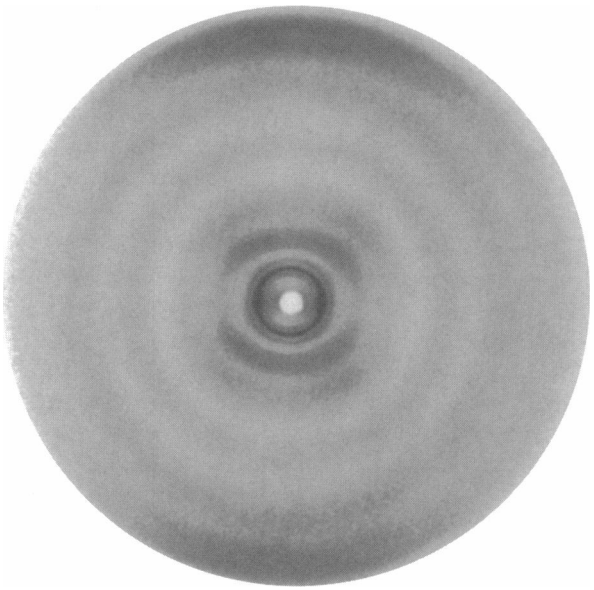

FIGURE 8 X-ray pattern typical of the phase with germs recorded at wavelength λ = 1.27 Å on an oriented 137 sample. This pattern is characteristic of DNA in the B form, with a meridian arc at 3.35 Å in its outer part. The hexagonal lateral order with interhelix distances of 29.85 Å is revealed by the sharp arc, with a strong equatorial reinforcement observed in the inner part of the pattern. The four other sharp and weak arcs suggest the presence of a beginning longitudinal order between neighboring DNA molecules.

cholesteric one. The scattered intensity $I(s)$ is shown on Fig. 7 for a biphasic sample. One observes sharp reflections due to the hexagonal phase and the broad peak characteristic of the cholesteric phase.

For samples 139 and 142, the parameters a_H and P, characteristic of the hexagonal phase, are very close to those found above in the phases with germs: $a_H = 29.85 \pm 0.05$ Å and $P = 34.7 \pm 0.3$ Å. The average interhelical spacing in the cholesteric part is slightly smaller than the pure cholesteric phase: $a_m = 31.6 \pm 0.3$ Å.

Conformation of the DNA molecule. As mentioned above, all x-ray patterns exhibit a diffuse ring located at 3.35 Å, which is usually observed for the B conformation of DNA. Moreover, it is possible to simulate the x-ray patterns by using the atom coordinates corresponding to the different potential conformations (A, B, or C). Such simulations show that only the use of the coordinates of the B form provides a satisfactory description of our patterns. Consequently, we can assume that the aggregation of DNA by spermidine does not change the secondary structure of the DNA molecule, which remains of the B type, whatever the nature of the spermidine-condensed DNA phase.

Stability of the phases

We performed three series of experiments to establish the thermodynamic stability of the different phases.

Temperature effects

The effects of temperature on the supramolecular organization of the condensed aggregates was investigated on a biphasic sample (point 143). The precipitate, corresponding to 89% of the total amount of DNA, is composed of about 80% hexagonal and 20% cholesteric phases, as estimated roughly in polarizing microscopy, at room temperature. We notice also the presence of isotropic droplets trapped in the precipitate.

The evolution of the samples with the temperature was followed in parallel in polarizing microscopy and by x-ray diffraction experiments. Both methods present interesting points and limitations.

First, a whole sample prepared in an Eppendorf tube was carefully sealed and submitted to a cycle of temperature ranging from 4 to 60°C in the following sequence: 2 h at 4°C, 2 h at 60°C, 1 h 30 at 25°C, 1 h at 4°C, 1 h at 60°C, and 1 h at 25°C. The aggregate was analyzed at the end of the cycle in polarizing microscopy; it was identical to a sample kept at room temperature. The amounts of cholesteric and hexagonal phases remained unchanged.

In addition, part of the aggregate was deposited between slide and coverslip. The preparation was sealed carefully and settled in a Mettler stage. The temperature was varied at a rate of 1 or 2°C/min from 20 to 65°C for a few cycles, and the experiment was repeated with different samples. When the temperature is raised, the germs progressively disappear in the cholesteric phase. The end of the transition occurs at about 45°C. It was not possible to determine very accurately the temperature at which there are no longer hexagonal germs, for several reasons: 1) It was impossible to deposit the whole sample (precipitate + supernatant) between slide and coverslip. Only the aggregate together with a small part of the supernatant was followed when varying the temperature, which may be slightly different from the first experiment. 2) In the aggregate, the two birefringent phases present a different viscosity and segregate. The germs tend to remain in the center of the preparation, and the cholesteric phase flows around to the periphery. Depending on the part of the preparation that was observed, the germs disappeared at slightly different temperatures. Therefore, the presence of the germs was checked in the whole preparation. However, we cannot be sure that the totality of the sedimented DNA was taken for the experiment. 3) Whatever resins we used to seal the coverslip, it happened that a slight dehydration occurred anyway. This effect was more noticeable the longer the time of the experiment. We therefore had to find a compromise between the dehydration process and the speed of temperature increase. A rate of 2°C/min was chosen.

In parallel with the transition from the hexagonal to the cholesteric phase, we also observed a transition from the cholesteric to an isotropic phase. Small dark droplets appeared in the birefringent cholesteric phase. They grew and merged. It is quite impossible to quantify the amount of this phase.

The pitch of the cholesteric phase was also shown to vary with temperature. A series of micrographs was taken during the course of the experiment, and the periodicity of the fingerprint patterns ($P_c/2$) was measured accurately on enlargements of the micrographs. $P_c/2$ varies from about 11.5 μm at 20°C to less than 2 μm at 65°C (Fig. 9). There is no significant hysteresis effect, as can be seen by comparing the data collected during the temperature increase and during the temperature decrease. At room temperature, the pitch was difficult to measure because it is quite large, usually leading to planar textures in thin preparations. Therefore, measurements were made in capillaries 1 mm in diameter after stabilization of the sample.

After 1 day at 65°C, the samples were still shown to present very beautiful cholesteric textures, indicating that the DNA molecule was not denatured and retained its double-stranded structure. Indeed, denatured DNA molecules no longer formed cholesteric liquid crystalline phases (Evdokimov et al., 1973). In our experimental conditions, two factors act simultaneously to increase the T_m of the DNA molecule: the presence of spermidine, which stabilizes the DNA double helix (Tabor, 1962), and the dense packing of the DNA molecules into an ordered liquid crystalline phase (Grasso et al., 1991).

Our microscopic data were completed by x-ray diffraction experiments on the same biphasic sample (point 143). The cycle of temperature was performed as follows: 25°C → 5°C → 65°C → 0°C → 25°C, proceeding by temperature steps of 4°C. For each step, the temperature was kept constant for about 2 h. The preparation remained biphasic at 5°C, but the intensity of the broad peak characteristic of the cholesteric phase was strongly lowered. During the temperature increase, the intensity of this peak rose again and the hexagonal structure completely disappeared at about 40°C. When the temperature was lowered, the reappearance of the germs was delayed, and a few become detectable at 20°C. The important point is that during the entire cycle of temperature, the parameter a_m of the cholesteric phase and those of the hexagonal phase (a_H and P) do not show a visible change.

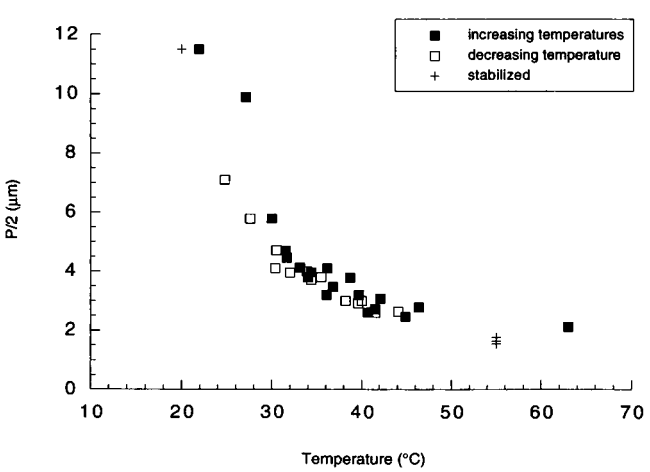

FIGURE 9 Variation of half the helical pitch $P_c/2$ of the cholesteric phase as a function of temperature. Full squares correspond to the increasing temperature range and empty squares to the decreasing temperature range. Half-pitches smaller than 2.45 μm ($T > 45$°C) remained unresolved with the 10× objective. Micrographs were therefore taken at a higher magnification immediately after the removal of the preparation from the Mettler stage. Crosses correspond to measurements done after stabilization of a few hours at a given temperature.

These experiments showed that the proportions of the different mesophases, their textures, and their crystallographic parameters remain unchanged after one or a few temperature cycles, thus showing that the transitions are reversible. The hexagonal phase disappears at a temperature close to 45°C.

Drying and resuspension of the sample in the mother liquor

Two series of experiments were performed:

After the supernatant was removed, a few DNA pellets were dried down in vacuum at 60°C for 2 h in a speed-vac chamber, further resuspended in their mother liquor, and left at room temperature for at least 1 day. Four different experimental points, corresponding to various natures of the aggregates (120, 111, 190, and 243) were tested twice this way. In all cases, the DNA aggregates recovered their original aspect, as seen in polarizing microscopy. Their crystallographic nature was not checked by x-ray diffraction analysis.

A small amount of the pellet (point 36) was deposited onto a slide and spread gently with a coverslip so as to prepare a smear, which was allowed to dry at 50°C for at least 1 h. The supernatant was added, and the evolution of the textures was followed in the polarizing microscope. This procedure allowed us to follow the sequence of events and to analyze the textures precisely. Upon drying, the aggregate turns solid and crystalline. The addition of the supernatant transforms it into an isotropic phase, which turns into a high-pitch cholesteric phase. In this phase it is possible to follow the growth of elongated domains that appear to be composed of aligned hexagonal germs (Fig. 5 *d*). Molecules are always normal to the elongation axis of the germ. The presence of numerous isotropic droplets was unambiguously observed during this experiment (Fig. 5 *d*). They align parallel to the elongated hexagonal domains. After they have merged together, their presence is not so easily detected. In other samples, where the dried pellet was resuspended vigorously with the supernatant, a network of these bubbles can be seen transiently.

Comparison of different preparation methods

Instead of adding spermidine to the 1 mg/ml aqueous DNA solution, precipitation was obtained by dilution of a concentrated solution (25 mg/ml DNA, 392 mM spermidine, and 250 mM NaCl) with TE buffer (10 mM Tris, pH 7, 6). DNA remains soluble in the concentrated solution and precipitates under a given spermidine concentration, as already

described by Becker et al. (1979). Dilution was either slow (rate of 10 μl/min) or fast (total volume of TE buffer added at one time). Three experimental points were chosen (16, 36, 190). Whatever the method used (addition of spermidine, fast dilution, and slow dilution), the amount of DNA sedimented in the pellet was the same, as was the nature of the pellet (checked in polarizing microscopy).

All of these approaches led us to the conclusion that we were dealing here with thermodynamically stable liquid crystalline phases, as explained briefly by Sikorav et al. (1994).

Concentration and dilution experiments

All experiments reported so far were done at a given DNA concentration, which was chosen to be 1 mg/ml. To be sure not to miss any crystalline or liquid crystalline phase in the whole phase diagram, another series of experiments was performed. The concentrations of the different components (DNA, NaCl, spermidine) were not kept constant, but varied either by dehydration or by dilution of the solution under the microscope. In this set of experiments, the ratio between DNA monovalent salts and spermidine was kept constant. These experiments were only qualitative.

Dilution experiments

Solutions of DNA and spermidine remain isotropic in the presence of a high concentration of monovalent salt. A dilution of the solution induces the aggregation of DNA by lowering the NaCl concentration, as reported previously (Damaschun et al., 1978; Becker et al., 1979). These data were used to follow under the microscope the formation of the birefringent aggregates, when drops of distilled water were added to a solution of DNA and spermidine. Reproducible results were obtained for various spermidine/DNA phosphate ratios (1, 5, 10).

When water is added, the clear solution suddenly turns foggy, and higher magnifications allowed us to recognize the presence of multiple microscopic birefringent droplets. They grow progressively and merge to form birefringent domains, which may sediment at the bottom of the cupel. When the amount of water is increased, the birefringent aggregates become denser. Instead of being added drop by drop, a large drop of distilled water (about 20 μl) can also be added at a time. In this manner, very elongated, dense fibers are suddenly formed. These fibers usually retract onto themselves in a few tens of seconds to form birefringent masses, which dissolve into the solution when the concentrations of the different components equilibrate. The analysis of these aggregates usually remains impossible as long as they remain floating in the solution. After their sedimentation and spreading at the bottom of the cupel, the textures can be analyzed.

The different phases described above were obtained easily with this method, whatever the spermidine/DNA phosphate ratio (1, 5, 10), namely the cholesteric phase and the germs of the columnar hexagonal phase. The preparations were sometimes thick enough to observe more easily than in thin preparations the characteristic patterns of the cholesteric phase (Fig. 10, *a* and *b*) and defect lines characteristic of this organization (Fig. 10 *a*).

The main attraction of this method was that it could be used to observe unstable structures not easily seen in the previous series of experiments. For low amounts of water, we observed reproducibly the formation of isotropic droplets in the birefringent phase (Fig. 10 *a*). These droplets become numerous and form a bubble network, and the birefringent phase is then confined to a thin film surrounding the isotropic droplets (Fig. 10, *c* and *d*). These structures appear rapidly and they are highly unstable—the droplets show a tendency to fuse together and to segregate from the birefringent phase. Such networks of isotropic bubbles in equilibrium with the cholesteric phase were also observed in the presence of 10 mM $MgCl_2$ (Fig. 10 *c*).

Dehydration experiments

In dehydration experiments, the isotropic DNA and spermidine solution was allowed to concentrate either in free surface drops or between slide and coverslip. We observed a transition to classical DNA liquid crystalline phases, first cholesteric with a small helical pitch (about 2.5 μm), and then columnar hexagonal (Fig. 10 *d*). These phases look similar to those described previously with DNA in the absence of spermidine (Leforestier and Livolant, 1991, 1993).

Phase diagram

In addition to the dilute isotropic solution, which contains from 4% to 85% of the total DNA (which corresponds to a concentration of 0.04 to 0.85 mg/ml), depending on the precipitation conditions, we observed two birefringent concentrated phases of DNA, sedimented in the pellet:

A cholesteric phase with a large helical pitch (22 μm). In this phase the interhelix distance varies from 31.6 to 32.6 ± 0.3 Å.

A hexagonal phase, showing a beginning of a longitudinal order along the axis of the DNA molecule. The interhelix distances are well defined in this phase: $d = 29.85 \pm 0.05$ Å, from which a DNA concentration of about 425 mg/ml can be calculated.

Polarizing observations and crystallographic data allow us to propose a phase diagram of the different states of condensed DNA, obtained in the presence of salt and spermidine for a given DNA concentration of 1 mg/ml (Fig. 11). For increasing salt and spermidine concentrations, we get first a hexagonal phase, then a biphasic domain (coexistence of cholesteric and columnar phases), and finally a pure cholesteric phase. The limits of the phase boundaries were extrapolated from the experimental points. All of these

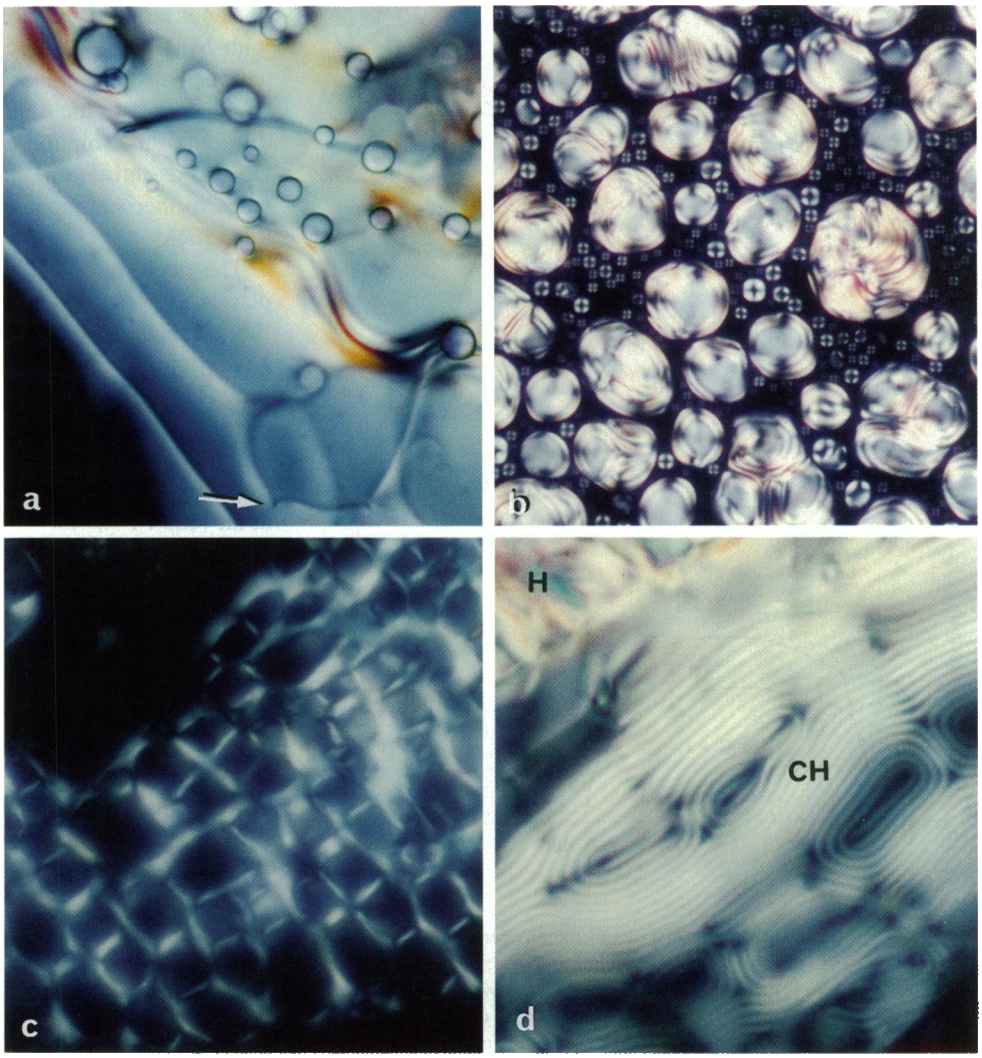

FIGURE 10 (*a–c*) Textures of the spermidine-DNA birefringent phases obtained by dilution with distilled water of a solution containing DNA and spermidine (with spermidine/DNA ratio = 1) in the presence of 25 mM NaCl and 10 mM $MgCl_2$. Dilution was performed in a cupel or in thick preparation between slide and coverslip. (*a*) Planar cholesteric textures, characterized by the presence of defect lines with cusp points (arrow). Note the presence of isotropic droplets. Crossed polars, ×400. (*b*) Cholesteric droplets in equilibrium with the dilute isotropic phase. Crossed polars, ×160. (*c*) Three-dimensional network of isotropic droplets in the cholesteric phase. Crossed polars, ×400. (*d*) Classical liquid crystalline phases of spermidine-DNA complexes, either cholesteric (CH) or columnar hexagonal (H). They were obtained after a progressive dehydration of the solution between slide and coverslip. Crossed polars, 2λ/4, ×1200.

concentrated phases are in equilibrium with the dilute isotropic DNA solution.

In the presence of 10 mM $MgCl_2$, the domain of existence of the condensed phases is reduced (Fig. 11 *b*), and we no longer observe the presence of a single columnar phase. Nevertheless, there is no significant difference due to the presence of these divalent cations; the phase diagram is simply displaced toward higher ionic concentrations. The pitch of the cholesteric phase is not significantly different in both cases (about 24 μm), but the presence of Mg^{2+} ions causes fingerprint textures to form instead of planar textures. This probably means that the monovalent and divalent cations influence the anchoring conditions of the DNA molecule on the glass surfaces; all orientations are permitted in the presence of Mg^{2+} ions, whereas a parallel orientation is preferred otherwise.

DISCUSSION

The liquid crystalline nature of polyamine-condensed DNA was hypothesized by several authors (Schellman and Parthasarathy, 1984; Damaschun et al., 1978) but never unambiguously established. Polarizing microscopy led us to determine that spermidine-DNA complexes condense into two different phases, and that at least one of them was fluid (Sikorav et al., 1994). The nature of these two phases is now established: a cholesteric phase with a large helical pitch, with interhelix distances ranging from 31.6 to 32.6 Å, and a columnar hexagonal phase with a restricted fluidity in which DNA molecules are more closely packed (29.85 ± 0.05 Å). The formation of these phases depends on the spermidine and NaCl concentrations, and their domain of existence is defined for a DNA concentration of 1 mg/ml. The effect of NaCl concentration on the nature of the spermine-DNA complexes was previously reported by Damaschun et al. (1978), who found that complexes show different circular dichroism spectra, either Ψ^+ in the presence of 0.075 mM NaCl or Ψ^- with 0.15 M NaCl. These two types of aggregates could correspond to the two liquid crystalline phases described here, which we also observed when DNA was condensed by spermine instead of spermidine (unpublished results).

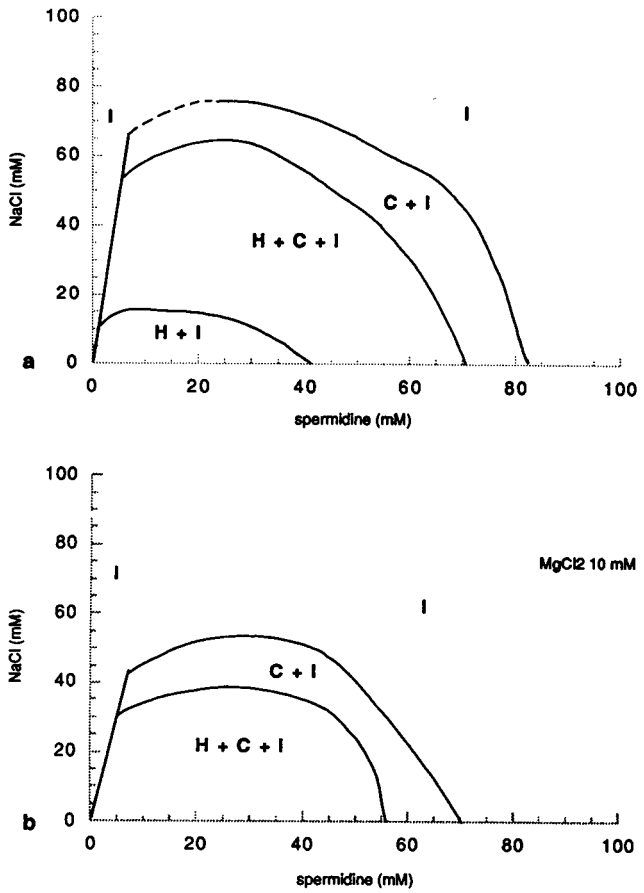

FIGURE 11 Schematic phase diagram of the different condensed DNA phases obtained in the presence of spermidine and salts: hexagonal (H) and cholesteric liquid crystalline (C). These phases are always in equilibrium with the dilute isotropic solution (I). (*a*) In the presence of monovalent salts (Na^+). The different regions (H, H + C, C) are sequentially observed for a parallel increase of Na^+ and spermidine concentrations. (*b*) In the presence of monovalent salts (Na^+) and 10 mM Mg^{2+} ions. There are only two different regions, H + C and C, also in equilibrium with the dilute isotropic phase I.

Comparison of the DNA mesophases obtained by dilution or by concentration of the sample

Two methods can be used to induce the transition from a dilute isotropic solution of DNA and spermidine to concentrated and ordered DNA mesophases while keeping constant the relative amounts of DNA, spermidine, and monovalent salts: either addition of water or dehydration of the solution. Both transitions are reversible, as schematically represented below:

	addition of water		*dehydration*	
Liquid crystalline phases (A)	← →	Isotropic solution (DNA + spermidine)	→ ←	Liquid crystalline phases (B)

By progressive dehydration of the sample, multiple liquid crystalline phases are obtained (B), namely a cholesteric phase with a helical pitch of about 2.5 μm and a columnar hexagonal phase (Fig. 10 *c*). The presence of spermidine does not modify the evolution that was analyzed previously with NaDNA (Durand et al., 1992). In these phases, interactions between molecules are net repulsive.

By contrast, the liquid crystalline phases obtained by dilution of the solution (A) correspond to the aggregation of DNA rods through net attractive interactions. These aggregates further sediment from the supernatant, as reported in this article.

The occurrence of these two types of liquid crystalline phases can be understood qualitatively in the frame of Flory's theory, which describes the behavior of rigid rods as a function of the quality of the solvent, characterized by the Flory-Huggins parameter χ (Flory, 1953, 1956). Liquid crystalline phases obtained by dehydration (B) or by dilution (A) would correspond to different solvent conditions χ, respectively, <0 (B) or >0 (A), as already stated by Sikorav et al. (1994).

In both cases, DNA forms cholesteric and columnar hexagonal phases, but they differ in several respects, as summarized in Table 2. The interhelix distances of the spermidine-condensed cholesteric phase (31.6 to 32.6 Å), although at the limit, remain in the range observed for the classical cholesteric phase. The high pitch (22 μm) indicates that the average twist angle between adjacent molecules is about 0.05° versus 0.46° in the concentrated classical cholesteric phase. The pitch may increase sometimes at the cholesteric-columnar boundary from 2.5 to 10 μm (Van Winkle et al., 1990, and our own observations), and this transition occurs when the interhelix distance reaches a value close to 31.5 Å (Durand et al., 1992). This increase in the pitch reveals a decrease in the average twist angle between neighboring molecules. We suggest that the high pitch observed in the spermidine-condensed DNA cholesteric phase may be due to the small distance separating the helices (between 31.6 and 32.6 Å), which would similarly prevent larger twist angles between adjacent molecules.

The columnar phase of the spermidine-condensed DNA shows intermolecular distances (29.85 ± 0.05 Å) close to the values found previously by Schellman and Parthasarathy

TABLE 2 Characteristics of cholesteric and two-dimensional hexagonal phases of DNA

	Liquid crystalline phases induced by spermidine (A)	Classical liquid crystalline phases (B)
Cholesteric phase	Cholesteric pitch P_c = 22 μm 31.6 Å < a_m < 32.6 Å	Cholesteric pitch P_c = 2.5 μm* 32 Å < a_m < 49 Å#
2D columnar hexagonal phase	a_H = 29.85 ± 0.05 Å	29 Å < a_H < 31.5 Å§
	DNA helical pitch P = 34.7 Å	DNA helical pitch 34.6 Å > P > 33.6 Å

*Leforestier and Livolant (1993).
#Strzelecka and Rill (1987), Strzelecka et al. (1988), Rill et al. (1991).
§Durand et al. (1992).

(1984) by x-ray diffraction analysis (29.4 to 29.55 Å). These values are in the range of distances measured in the classical two-dimensional columnar hexagonal phase. In contrast, the fluidity of the edifice is strongly reduced and there is the beginning of a longitudinal order along the direction of the molecules. This longitudinal ordering may explain the differences in the textures, namely the absence of curvature of the columns in the DNA mesophase induced by spermidine.

Furthermore, in classical liquid crystalline phases, the distance between DNA helices was shown to decrease progressively from 29 to 49 Å when the preparation was slowly dehydrated, with a transition from two-dimensional columnar hexagonal to cholesteric at an interhelix spacing of 31.5 Å (Durand et al., 1992). In liquid crystalline phases induced by spermidine, only two ranges of interhelix distances are found and they are precisely defined: 31.6 to 32.6 Å in the cholesteric phase and 29.85 ± 0.05 Å in the columnar phase. Intermediate values cannot be obtained whatever the spermidine and sodium chloride concentrations. Instead, it is the relative amount of both phases that is modulated. We assume that these two ranges of interhelix distances correspond to two equilibrium values in the balance between the attractive and repulsive interactions between DNA helices.

Precipitation and suppression of precipitation

In our experiments, we confirmed that the condensation of DNA induced by the addition of spermidine occurs over a short range of concentration, as previously discussed (Osland and Kleppe, 1977; Bloomfield, 1991), but also that this precipitation can be suppressed by increasing the monovalent salt concentration (Heby and Agrell, 1971) or by raising the spermidine concentration. We did not find a simple relationship between the amount of DNA precipitated in the pellet and the nature of the condensed DNA phase. This aspect is illustrated in Fig. 6: a precipitation of about 95% DNA may correspond either to a pure hexagonal phase (15 mM spermidine, NaCl 4 mM) or to a pellet that is mainly cholesteric (20 mM spermidine, 25 mM NaCl). Nevertheless, when the amount of sedimented DNA is small, the phase is usually not hexagonal. Any increase in the ionic strength of the solution, in NaCl, $MgCl_2$, or spermidine, tends to favor the cholesteric phase.

The condensation of DNA by multivalent cations is a large and complex field that is far from being completely elucidated (see Bloomfield et al., 1994, for a review). Electrostatic forces are known to play a significant role, as demonstrated by Wilson and Bloomfield (1979), who showed that condensation of DNA occurs under a wide range of ionic conditions, inasmuch as 89% to 90% of the charges of the DNA molecule are neutralized by counterion condensation of multivalent and monovalent counterions. These results pointed out the importance of the suppression of electrostatic repulsion in the process of condensation. However, our data, showing that between DNA helices there are two ranges of equilibrium distances, that these distances are independent of the ionic environment (either in monovalent or trivalent cations), and that suppression of DNA precipitation can be obtained by increasing NaCl but also spermidine concentrations, cannot be explained by a balance of repulsive electrostatic forces and attractive Van der Waals interactions. Net attractive interactions could be generated by fluctuations in the trivalent ion distribution around the DNA molecules, as first proposed by Oosawa (1971), and this attraction could be strong enough to stabilize DNA in a condensed state (Marquet and Houssier, 1991).

The other forces possibly involved in the stabilization of the DNA aggregates are cross-links by condensing counterions (Schellman and Parthasarathy, 1984) and hydration forces (Rau and Parsegian, 1992). Using spermidine analogs of the structure NH_3^+-$(CH2)_3$-NH_2^+-$(CH_2)_n$-NH_3^+ with n = 3, 4, 5, and 8 to collapse DNA, Schellman and Parthasarathy found that the interhelix spacing was a monotonous increasing function of the chain length and that the ionic strength of the solution had no effect on the spacing, suggesting that the arrangement of DNA in the complexes was determined by the structure of the polycation. Our experimental data argue against this cross-linking hypothesis, because we obtained different spacings of the DNA molecules with a unique polycation (spermidine), showing that the correlation between spacing and ion size no longer holds. Rau and Parsegian (1992) postulated the existence of hydration structure forces. They expect these forces to be of importance when the interhelix distance is smaller than 30–35 Å, the range of interhelix distances that we are dealing with here (29.8 to 32.6 Å). Nevertheless, we cannot make decisive arguments supporting the existence of these hydration forces.

To clarify the understanding of these phenomena, more experimental work comparing the effect of different multivalent ions on DNA condensation has been undertaken (Pelta et al., 1996). Nevertheless, the nature of the forces involved in the aggregation of DNA by trivalent cations remains to be understood.

Functional properties of spermidine-condensed chromatin

In vitro, polyamines are frequently used to stimulate the functional properties of DNA molecules, and numerous examples of such effects were reported previously (Sikorav et al., 1994), showing that the efficiency of replication, transcription, homologous pairing of DNA strands, DNA renaturation, cleavage by restriction enzymes, and catenation of DNA by topoisomerases can be significantly increased by the addition of spermidine. In a few cases a correlation between condensation of DNA and stimulation of the functional properties of the DNA molecules was demonstrated (Gonda and Radding, 1986; Krasnow and Cozzarelli, 1982), and we suggested that the liquid crystal-

line nature of the spermidine-condensed state was probably of great importance to the increase in this activity. Moreover, as illustrated by the present results, condensation of DNA is not an all-or-none process, and a large polymorphism of structural organization of DNA can be obtained by slightly varying the amount of spermidine, NaCl, and water, while keeping the B secondary structure of the molecule. How this polymorphism could be essential in the regulation of the genetic activity can be illustrated by a previous work in which the transcriptional activity of the pBr322 DNA molecule (with *E. coli*-dependent RNA polymerase) was followed in parallel with the condensation of the molecule by spermidine (Baeza et al., 1987). Transcription activity of DNA molecule was practically the same in the absence of spermidine and with a concentration of spermidine below the concentration required to induce condensation. At the lowest concentration of spermidine that caused DNA condensation, about a 90-fold increase in transcription was observed, whereas larger amounts of spermidine, which form more compact structures, cause only a fourfold increase in transcription. DNA condensation and significant increase in the transcription activity were simultaneously canceled by increasing the ionic strength. We may assume that the pBr 322 molecule was forming an intramolecular liquid crystal (as proposed by Grosberg and Khokhlov (1981) with an external toroidal shape, which was either cholesteric (moderate condensation and high activity) or columnar hexagonal (high condensation and moderate activity). The cholesteric organization, which allies molecular ordering and high fluidity, can be easily understood as being more favorable for the transcriptional activity of the molecule.

In the cell, spermidine acts in competition with other condensing agents such as histone proteins to regulate the supramolecular organization of DNA, and through this condensing action is involved in the regulation of numerous biological functions.

We warmly acknowledge Jean-Louis Sikorav for many fruitful discussions, namely about the functional properties of spermidine-condensed DNA.

This work was supported by grants from the Association pour la Recherche sur le Cancer (ARC 6473) and from the Ministère de l'Enseignement Supérieur et de la Recherche (DSPT5 and ACC-SV5).

REFERENCES

Baeza, I., P. Gariglio, L. M. Rangel, P. Chavez, L. Cervantes, C. Arguello, C. Wong, and C. Montanez. 1987. Electron microscopy and biochemical properties of polyamine-compacted DNA. *Biochemistry.* 26:6387–6392.

Becker, M., R. Misselwitz, H. Damaschun, G. Damaschun, and D. Zirwer. 1979. Spermine-DNA complexes build up metastable structures. Small-angle x-ray scattering and circular dichroism studies. *Nucleic Acids Res.* 7:1297–1309.

Bloomfield, V. A. 1991. Condensation of DNA by multivalent cations: considerations on mechanisms. *Biopolymers.* 31:1471–1481.

Bloomfield, V. A., C. Ma, and P. G. Arscott. 1994. Role of multivalent cations in condensation of DNA. *In* Macro-ion Characterization: From Dilute Solution to Complex Fluids. ACS Symposium Series 548. K. S. Schmitz, editor. American Chemical Society, Washington, DC. 195–209.

Bouligand, Y. 1974. Recherches sur les textures des états mésomorphes. 6-Dislocations coins et signification des cloisons de Grandjean-Cano dans les cholestériques. *J. Phys.* 35:959–981.

Chattoraj, D. K., L. C. Gosule, and J. A. Schellman. 1978. DNA condensation with polyamines. II. Electron microscopic studies. *J. Mol. Biol.* 121:327–337.

Damaschun, H., G. Damaschun, M. Becker, E. Buder, R. Misselwitz, and D. Zirwer. 1978. Study of DNA-spermine interactions by use of small-angle and wide-angle x-ray scattering and circular dichroism. *Nucleic Acids Res.* 5:3801–3809.

Durand, D., J. Doucet, and F. Livolant. 1992. A study of the structure of highly concentrated phases of DNA by X-ray diffraction. *J. Phys. II.* 2:1769–1783.

Evdokimov, Y. M., N. M. Akimenko, N. E. Glukhova, A. S. Tikhonenko, and Y. M. Varshavsky. 1973. Production of the compact form of double-stranded DNA in solution in the presence of poly(ethylene)glycol. *Mol. Biol.* 7:151–159.

Evdokimov, Y. M., S. G. Skuridin, and V. I. Salyanov. 1988. The liquid-crystalline phases of double-stranded nucleic acids in vitro and in vivo. *Liquid Crystals.* 3:1443–1459.

Flory, P. J. 1953. Principles of Polymer Chemistry. Cornell University Press, Ithaca, NY.

Flory, P. J. 1956. Phase equilibria in solutions of rod-like particles. *Proc. R. Soc. Lond. A.* 234:73–89.

Gonda, D. K., and C. M. Radding. 1986. The mechanism of the search for homology promoted by recA protein. *J. Biol. Chem.* 261:13087–13096.

Gosule, L. C., and J. A. Schellman. 1976. Compact form of DNA induced by spermidine. *Nature.* 259:333–335.

Grasso, D., S. Fasone, and C. La Rosa. 1991. A calorimetric study of the different thermal behaviour of DNA in the isotropic and liquid crystalline states. *Liquid Crystals.* 9:299–305.

Grosberg, A. Yu., and A. R. Khokhlov. 1981. Statistical theory of polymeric lyotropic liquid crystals. *Adv. Polym. Sci.* 41:53–97.

Guinier A. 1956. Théorie et Technique de la Radiocristallographie. Dunod, Paris. 602.

Heby, O., and I. Agrell. 1971. Observations of the affinity between polyamines and nucleic acids. *Hoppe Seylers Z. Physiol. Chem.* 352:29–38.

Krasnow, M. A., and N. R. Cozzarelli. 1982. Catenation of DNA rings by topoisomerases. *J. Biol. Chem.* 257:2687–2693.

Leforestier, A., and F. Livolant. 1993. Supramolecular ordering of DNA in the cholesteric liquid crystalline phase: an ultrastructural study. *Biophys. J.* 65:56–72.

Leforestier, A., and F. Livolant. 1994. DNA liquid crystalline blue phases. Electron microscopy evidence and biological implications. *Liquid Crystals.* 17:651–658.

Lerman, L. S. 1974. Chromosomal analogues: long range order in ψ condensed DNA. *Cold Spring Harb. Symp. Quant. Biol.* 38:59–73.

Lerman, L. S., L. S. Wilkinson, J. H. Venable, and B. H. Robinson. 1976. DNA packing in single crystals inferred from freeze-fracture-etch replicas. *J. Mol. Biol.* 108:271–293.

Livolant, F. 1986. Cholesteric liquid crystalline phases given by three helical biological polymers: DNA, PBLG and xanthan. A comparative analysis of their textures. *J. Phys.* 47:1605–1616.

Livolant, F. 1987. Precholesteric liquid crystalline states of DNA. *J. Phys.* 48:1051–1068.

Livolant, F. 1991. Supramolecular organization of double-stranded DNA molecules in the columnar hexagonal liquid crystalline phase. *J. Mol. Biol.* 218:165–181.

Livolant, F., and Y. Bouligand. 1986. Liquid crystalline phases given by helical biological polymers (DNA, PBLG and XANTHAN). Columnar textures. *J. Phys.* 47:1813–1827.

Livolant, F., A. M. Levelut, J. Doucet, and J. P. Benoit. 1989. The highly concentrated liquid crystalline phase of DNA is columnar hexagonal. *Nature.* 339:724–726.

Luzzati, V., and A. Nicolaieff. 1959. Etude par diffusion des rayons X aux petits angles des gels d'acides desoxyribonucléiques et de nucléoprotéines. *J. Mol. Biol.* 1:127–133.

Luzzati, V., and A. Nicolaieff. 1963. The structure of nucleohistones and nucleoprotamines. *J. Mol. Biol.* 7:142–163.

Maniatis, T., J. H. Venable, and L. S. Lerman. 1974. The structure of ψ DNA. *J. Mol. Biol.* 84:37–64.

Manning, G. S. 1978. The molecular theory of polyelectrolyte solutions with applications to the electrostatic properties of polynucleotides. *Q. Rev. Biophys.* 11:179–246.

Marquet, R., and C. Houssier. 1991. Thermodynamics of cation-induced DNA condensation. *J. Biomol. Struct. Dyn.* 9:159–167.

Minton, A. P. 1981. Excluded volume as a determinant of macromolecular structure and reactivity. *Biopolymers.* 20:2093–2120.

Oosawa, F. 1971. Polyelectrolytes. Marcel Dekker, New York.

Osland, A., and K. Kleppe. 1977. Polyamine induced aggregation of DNA. *Nucleic Acids Res.* 1:685–695.

Pelta, J., F. Livolant, and J.-L. Sikorav. 1996. DNA aggregation induced by polyamines and cobalthexamine. *J. Biol. Chem.* 271:5656–5662.

Podgornik, R., H. H. Strey, K. Gawrisch, D. C. Rau, A. Rupprecht, and V. A. Parsegian. 1996. Bond orientational order, molecular motion and free energy of the high density DNA mesophases. *Proc. Natl. Acad. Sci. USA.* 93:4261–4266.

Rau, D. C., B. Lee, and V. A. Parsegian. 1984. Measurement of the repulsive force between polyelectrolyte molecules in ionic solution: hydration forces between parallel DNA double helices. *Proc. Natl. Acad. Sci. USA.* 81:2621–2625.

Rau, D. C., and V. A. Parsegian. 1992. Direct measurement of the intermolecular forces between counterion-condensed DNA double helices. Evidence for long range attractive hydration forces. *Biophys. J.* 61: 246–259.

Rill, R. L., T. E. Strzelecka, M. W. Davidson, and D. H. Van Winkle. 1991. Ordered phases in concentrated DNA solutions. *Phys. A.* 176:87–116.

Robinson, C. 1961. Liquid-crystalline structures in polypeptide solutions. *Tetrahedron.* 13:219–234.

Schellman, J. A., and N. Parthasarathy. 1984. X-ray diffraction studies on cation-collapsed DNA. *J. Mol. Biol.* 175:313–329.

Sikorav, J. L., J. Pelta, and F. Livolant. 1994. A liquid crystalline phase in spermidine-condensed DNA. *Biophys. J.* 67:1387–1392.

Strzelecka, T. E., M. W. Davidson, and R. L. Rill. 1988. Multiple liquid crystalline phases of DNA at high concentrations. *Nature.* 331:457–460.

Strzelecka, T. E., and R. L. Rill. 1987. Solid-state ^{31}P NMR studies of DNA liquid crystalline phases. The isotropic to cholesteric transition. *J. Am. Chem. Soc.* 109:4513–4518.

Tabor, H. 1962. The protective effect of spermine and other polyamines against heat denaturation of deoxyribonucleic acid. *Biochemistry.* 1:496–501.

Tabor, C. W., and H. Tabor. 1984. Polyamines. *Annu. Rev. Biochem.* 53:749–790.

Vainshtein, B. K. 1966. Diffraction of X-ray by Chain Molecules. Elsevier Publishing Company, Amsterdam, London, New York.

Van Winkle, D. H., M. W. Davidson, W. X. Chen, and R. L. Rill. 1990. The cholesteric helical pitch of near persistence length DNA. *Macromolecules.* 23:4140.

Wilson, R. W., and V. A. Bloomfield. 1979. Counterion-induced condensation of deoxyribonucleic acid. A light-scattering study. *Biochemistry.* 18:2192–2196.